Jain, H.V., Meyer-Hermann, M.

The molecular basis of synergism between carboplatin and ABT-737 therapy targeting ovarian carcinomas
(2011) Cancer Research, 71 (3), pp. 705-715

Published OnlineFirst December 17, 2010; DOI: 10.1158/0008-5472.CAN-10-3174

Cancer Research

The Molecular Basis of Synergism between Carboplatin and ABT-737 Therapy Targeting Ovarian Carcinomas

Harsh Vardhan Jain[1] and Michael Meyer-Hermann[2,3]

Abstract

Resistance to standard chemotherapy (carboplatin + paclitaxel) is one of the leading causes of therapeutic failure in ovarian carcinomas. Emergence of chemoresistance has been shown to be mediated in part by members of the Bcl family of proteins including the antiapoptotic protein Bcl-x_L, whose expression is correlated with shorter disease-free intervals in recurrent disease. ABT-737 is an example of one of the first small-molecule inhibitors of Bcl-2/Bcl-x_L that has been shown to increase the sensitivity of ovarian cancer cells to carboplatin. To exploit the therapeutic potential of these two drugs and predict optimal doses and dose scheduling, it is essential to understand the molecular basis of their synergistic action. Here, we build and calibrate a mathematical model of ABT-737 and carboplatin action on an ovarian cancer cell line (IGROV-1). The model suggests that carboplatin treatment primes cells for ABT-737 therapy because of an increased dependence of cells with DNA damage on Bcl-x_L for survival. Numerical simulations predict the existence of a threshold of Bcl-x_L below which these cells are unable to recover. Furthermore, co- plus posttreatment of ABT-737 with carboplatin is predicted to be the best strategy to maximize synergism between these two drugs. A critical challenge in chemotherapy is to strike a balance between maximizing cell-kill while minimizing patient drug load. We show that the model can be used to compute minimal doses required for any desired fraction of cell kill. These results underscore the potential of the modeling work presented here as a valuable quantitative tool to aid in the translation of novel drugs such as ABT-737 from the experimental to clinical setting and highlight the need for close collaboration between modelers and experimental scientists. *Cancer Res; 71(3); 705–15. ©2010 AACR.*

Major Findings

The reduced ability of DNA-damaged cancer cells to withstand changes in intracellular Bcl-xL concentration is predicted to be the principle reason behind the observed synergism between carboplatin and ABT-737. This suggests co- plus post-treatment of tumors by ABT-737 with carboplatin as the optimal strategy to maximize cell-kill, whilst minimizing patient drug load.

Introduction

Ovarian cancer is the fifth most common cause of cancer death in women in the developed world. Although progress has been made in its treatment with the introduction of platinum-taxane–based chemotherapy since the 1980s, the mortality rate remains largely unchanged in the past 2 decades (1). The overall 5-year survival rate is only 29%, possibly due to infrequent early diagnosis coupled with the emergence of drug resistance in recurrent disease (2). The current gold standard for chemotherapy targeting ovarian cancer is a combination of carboplatin, a platinum-based compound, together with paclitaxel, an antimitotic drug. In fact, a majority of patients respond well to this treatment initially. However, most will suffer relapse following complete clinical response and the emergence of drug resistance is observed in a majority of these cases, implying an overall poor prognosis (3).

Several factors may contribute to this drug resistance, including decreased drug uptake by and/or increased efflux from cancer cells, increased rate of drug-induced DNA damage repair, loss of p53 function, and protection from apoptosis (3, 4). In particular, ectopic expression of the apoptosis inhibitor protein Bcl-x_L has been linked to drug resistance. Bcl-x_L is a member of the Bcl-2 family of intracellular proteins that are crucial regulators of programmed cell death (5). In ovarian cancers, Bcl-x_L expression in primary tumors is associated with shorter disease-free intervals following successive bouts of chemotherapy (6). Furthermore, *in vitro* studies have shown that overexpression of Bcl-x_L confers resistance to cell death induced by a variety of chemotherapeutic agents including cisplatin (a carboplatin analogue), and paclitaxel (6–8).

Authors' Affiliations: [1]Mathematical Biosciences Institute, The Ohio State University, Columbus, Ohio; [2]Department of Systems Immunology, Helmholtz Centre for Infection Research (HZI), Braunschweig, Germany; and [3]Frankfurt Institute for Advanced Studies (FIAS), Frankfurt am Main, Germany

Note: Supplementary data for this article are available at Cancer Research Online (http://cancerres.aacrjournals.org/).

Corresponding Author: Michael Meyer-Hermann, Helmholtz Centre for Infection Research (HZI), Inhoffenstr. 7, 38124 Braunschweig, Germany. Phone: 49-151-52726087; Fax: 49-531-6181-7099; E-mail: michael.meyer-hermann@helmholtz-hzi.de

doi: 10.1158/0008-5472.CAN-10-3174

Published OnlineFirst December 17, 2010; DOI: 10.1158/0008-5472.CAN-10-3174

Quick Guide to Main Model Equations

The model schematic for tumor cell growth inhibition mediated by application of carboplatin and ABT-737 is presented in Fig. 1. The following is a brief description of the principal equations and underlying assumptions that drive this reaction diagram. Here, N and M refer to proliferating and arrested tumor cell numbers per well (ovarian cancer cell line IGROV-1), respectively. B, C, X, and P are total unbound Bcl-x_L, carboplatin, free ABT-737, and Bcl-x_L–ABT-737 complex concentration in micromoles per well, respectively. For a detailed description of the model and various terms, we refer the reader to the Supplementary Material.

$$\frac{dN}{dt} = \lambda_n N - \delta_n(b)N - \alpha(C)N + M(t, a = a_r) \quad \text{(A)}$$

This equation models the growth of proliferating IGROV-1 tumor cells in conditioned growth medium, *in vitro*, as described in ref. 11. Therapy is provided in the form of carboplatin (C) and ABT-737 (X) alone, or in combination. Tumor cells proliferate at a constant rate, λ_n, whereas their rate of death δ_n is mediated by the amount of free Bcl-x_L per cell, b. Note that $b = B/T$, where $T = N(t) + \int_0^t M(t,a)da$ is the total number of IGROV-1 cells at any time t. Furthermore, in response to carboplatin therapy, proliferating cells undergo cell-cycle arrest at a rate, α, dependent on the amount of carboplatin administered, C.

Major Assumptions of the Model

Assumption on apoptosis control

To keep the number of unknown parameters at a minimum, proapoptotic members of the Bcl family are not included in our model; instead, cell survival is assumed to depend on free Bcl-x_L, which, in conjugation with its proapoptotic counterparts and its free concentration per cell, is taken into account while estimating parameters relating to Bcl-x_L dynamics (See Table 1 and Supplementary Material, Section B2).

Assumption on arrested cell recovery

An additional source term for N is $M(t, a = a_r)$. This represents cells that are able to recover from carboplatin-induced DNA damage, with some characteristic recovery time a_r, and is described in Equation (B).

$$\frac{\partial M}{\partial t} + \frac{\partial M}{\partial a} = -\delta_m[b, C(t-a), a]M$$

Arrested IGROV-1 cells undergo apoptosis in an age-structured manner (a is the age variable), with death rate δ_m proportional to the amount of carboplatin present at the time of cell-cycle arrest [$C(t-a)$] and the amount of unbound Bcl-x_L per cell, b. The following boundary condition is imposed on this equation:

$$M(t, 0) = \alpha(C)N \quad \text{(B)}$$

This is a source term for M, which corresponds to the rate of cell-cycle arrest α of proliferating cells in Equation (A).

Assumption on DNA repair

On the basis of experimental observations in ref. 11, it is assumed that arrested cells begin to undergo apoptosis approximately 16 hours after the application of carboplatin. This time of onset of death may be reduced if free Bcl-x_L levels are lowered because of the application of ABT-737. The delay of 16 hours is explained by the sequence of events that follow DNA damage, including damage recognition, followed by DNA repair or eventual cell death. A detailed review of these events is presented in ref. 21. Furthermore, on the basis of experimental observations in ref. 11, it is assumed that the arrested cells that have not undergone apoptosis after 48 hours recover to the proliferating population. In the absence of data by which to estimate a rate of recovery, it is taken to occur instantaneously at the end of this time period. Thus, a_r is taken to have a value of 48 hours.

Assumption on carboplatin degradation

Following ref. 31, the rate of carboplatin decay in culture medium is assumed to obey the first-order kinetics.

$$\frac{dC}{dt} = -\lambda_c(C) \quad \text{(C)}$$

In ref. 31, *in vitro* cell proliferation assays of Jurkat cells cultured in the presence of carboplatin showed that for cell concentrations below 10^7 per mL, the rate of decay λ_c of carboplatin was unaffected by the presence of cells and was in fact approximately linear. In the experimental conditions relevant to our model, IGROV-1 cell numbers do not exceed 10^6 per mL.

Assumption on free Bcl-x_L

The rate of change of free intracellular Bcl-x_L concentration is modeled by

$$\frac{dB}{dt} = \gamma(b)T - \lambda_b B + \lambda_n N b_s - \delta_n(b)bN - b\int_0^t \delta_m(b, C(t-a), a)M\,da - k_1 BX + K_{-1}P \quad \text{(D)}$$

Bcl-x_L is produced by all tumor cells at a rate γ that depends on the current amount of Bcl-x_L per cell b. It undergoes natural decay at a rate λ_b. When a new cell is added as a result of proliferation, it is assumed to instantaneously establish a constitutive

Published OnlineFirst December 17, 2010; DOI: 10.1158/0008-5472.CAN-10-3174

level b_s of expression of free Bcl-x_L. This represents an addition to the total Bcl-x_L concentration B at the rate $\lambda_n N b_s$, whereas cell death in both proliferating and arrested cell populations results in the loss of Bcl-x_L. The integral term in the rate of loss of Bcl-x_L due to arrested cell death reflects the fact that apoptosis in cells of all ages in this compartment must be accounted for. Finally, free Bcl-x_L may interact with its small molecule inhibitor ABT-737 (X) to form complexes (P), where k_1 is the forward rate of the reaction $B + XP$ and k_{-1} is the backward rate.

Assumption on ABT-737 dynamics

The dynamics of free ABT-737 concentration in cell culture medium is given by

$$\frac{dX}{dt} = -\lambda_x X - k_1 BX + k_{-1} P \quad \text{(E)}$$

ABT-737 undergoes decay at a rate λ_x, corresponding to its natural half-life. Given the small size of small molecule inhibitors such as ABT-737 and their large permeability through cell membrane, it is assumed that ABT-737 is free to move in and out of cells, and when inside cells, it rapidly forms complexes P with Bcl-x_L.

Conversely, inhibition of Bcl-x_L expression with transfection by *bcl-x$_S$* (9), small interfering RNA (siRNA; refs. 10, 11), or a monoclonal antibody (ABT-737; ref. 11) increases sensitivity of ovarian cancer cell lines to these chemotherapeutic agents. It may therefore be concluded that concomitant inhibition of Bcl-x_L with chemotherapy could be an attractive treatment strategy for this cancer type (10, 11).

Witham and colleagues assess the therapeutic potential of cotreatment of an ovarian cancer cell line (IGROV-1) expressing Bcl-x_L with ABT-737 and carboplatin (11). ABT-737 belongs to a class of compounds that are nonpeptidic small molecule inhibitors of Bcl-x_L/Bcl-2 proteins and has been shown to exhibit significant single-agent activity against small cell lung carcinoma tumor xenografts in mice (12). It acts by blocking the Bcl-x_L–BH3 binding groove, which prevents it from sequestering proapoptotic members of the Bcl-2 family such as Bad, Bid, and Bim (13). According to Witham and colleagues (11), ABT-737 shows modest cytotoxic activity as a single-agent in *in vitro* cell proliferation assays of IGROV-1 cells. However, when given in combination with carboplatin, an increase in cell growth inhibition, coupled with a decrease in time to apoptosis, is observed. In fact, the relative timing of scheduling of the two drugs plays an important role in determining therapy efficacy. Posttreatment of cells with ABT-737, following treatment with carboplatin, is predicted to be the best strategy, indicating that carboplatin sensitizes the cells to anti-Bcl-x_L therapy. Finally, IGROV-1 tumor xenografts in mice are shown to respond equally well to the 2 drugs delivered alone, whereas therapy efficacy is greatly enhanced when the drugs are given in combination.

Although these findings have the potential of representing a significant advance in the treatment of ovarian cancers, an important step in the realization of these therapies is to develop an understanding of the molecular basis of synergism between such drugs. Evaluating key parameters such as the degree of synergism and optimization of chemotherapeutic schedules can be time consuming and costly. Quantitative modeling such as that described in this article has the potential to answer these questions while providing further insights into the mechanism of action of these therapies. We have previously developed models of tumor growth (14–16) and evaluated the therapeutic potential of small molecule inhibitors of Bcl-2 as antiangiogenic agents (17, 18). In this article, we present a multiscale model, with age structure of combination chemotherapy and anti-Bcl-x_L therapy targeting ovarian carcinomas, that is validated by direct comparison with experimental results taken from Witham and colleagues (11). Using this, we are able to provide a quantitative justification for the hypothesis that carboplatin sensitizes cancer cells to ABT-737. We propose an optimal dosing regimen for carboplatin and ABT-737 and thus provide a useful tool to make predictions relating to treatment protocols for drugs that are similar in action to these compounds.

Materials and Methods

Model foundation

To capture the relevant intracellular dynamics of Bcl-x_L–controlled cell apoptosis, a biochemically motivated ordinary differential equation model was developed. This was linked to a population-level model describing cell culture growth dynamics. An age structure was imposed on this to accurately simulate carboplatin-induced DNA damage and subsequent cell death. A model schematic detailing the effects of carboplatin and ABT-737 on a population of ovarian cancer (IGROV-1) cells is shown in Fig. 1. The choice of this particular cell line is based on the experiments described in ref. 11, wherein IGROV-1 cells were shown to specifically express high levels of Bcl-x_L while expressing little or no Bcl-2. Furthermore, they exhibited maximum sensitivity to ABT-737 as a single agent.

The following sections describe the principles underlying our model formulation. All simulations of the model were carried out on Matlab. The simulation methodology is described in greater detail in Supplementary Material, Section C.

Bcl-x_L as a regulator of cell death

IGROV-1 cells have been shown to grow exponentially (19) in the time frame of interest to us (the experiments described in ref. 11) were conducted over an average of 4 to 5 days. We therefore assume an exponential growth for IGROV-1 cells in the absence of therapy, as shown in Fig. 1A. The intrinsic

Published OnlineFirst December 17, 2010; DOI: 10.1158/0008-5472.CAN-10-3174

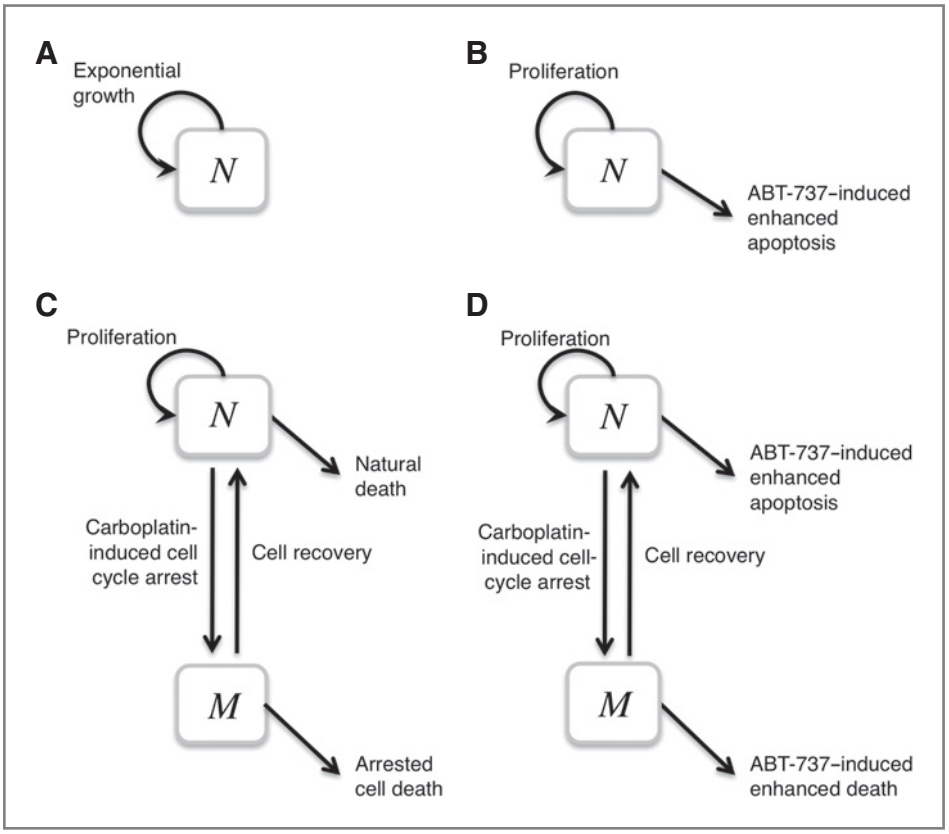

Figure 1. Model schematic. A, IGROV-1 cells are assumed to grow exponentially when cultured in the presence of growth medium and in the absence of any therapy. B, in the case wherein IGROV-1 cells are treated with ABT-737 alone, cell death rate is taken to be a function of intracellular free Bcl-x_L level (not shown), which will be decreased upon the application of ABT-737. C, in the case wherein IGROV-1 cells are treated with carboplatin alone, they undergo cell-cycle arrest at a rate dependent on the amount of drug delivered. The arrested cells subsequently undergo apoptosis at a rate proportional to the amount of drug present at the time of arrest. This occurs in an age-dependent fashion to account for experimentally observed time lag between therapy administration and PARP cleavage leading to cell death. Recovery of arrested cells to the proliferating population is also accounted for. D, in the case wherein IGROV-1 cells are treated with carboplatin and ABT-737 in combination, the two modules described in B and C previously are put together, with arrested IGROV-1 cell death rate and time to onset of death now a function of Bcl-x_L levels.

growth rate of the cells is fit to cell proliferation data taken from ref. 19, as shown in Fig. 2A.

Next, we include in our model, the regulation of cellular apoptosis controlled by Bcl-x_L, a schematic for which is shown in Fig. 1B. The intrinsic growth rate of IGROV-1 cells estimated earlier is divided into a constant proliferation rate, λ_n, together with a death rate that is taken to be a function of unbound Bcl-x_L concentration per cell. Choosing the death rate in this manner allows us to avoid estimating intracellular levels for a number of proteins and binding parameters, for which little or no experimental data are available. Furthermore, ABT-737 shows specific activity against Bcl-x_L and Bcl-2 (12), of which IGROV-1 cells do not express Bcl-2 (11). Therefore, it is reasonable to assume that changes in intracellular Bcl-x_L induced by ABT-737 would contribute to cell death in this experimental setup.

To model the effect of application of ABT-737 therapy, its concentration (X) is tracked in time, together with the concentration of Bcl-x_L summed over all cells (B). In the absence of experimental data detailing the mechanism of entry of small molecule inhibitors into the cell, it is assumed that ABT-737 is free to move in and out of the cell, and once inside the cell, it complexes rapidly with Bcl-x_L. This is a reasonable assumption, as these small molecule inhibitors are designed to be cell wall permeable. The law of mass action is used to translate the binding reaction between ABT-737 and Bcl-x_L into a system of differential equations that govern the temporal dynamics of these molecules (20).

The precise functional form for the death rate of proliferating cells is chosen by conducting fits of the model to *in vitro* cell growth inhibition data taken from ref. 11, wherein ABT-737 therapy is applied singly to IGROV-1 cell cultures (see Fig. 2B). The resultant rate reflects the fact that a drop in the levels of Bcl-x_L, possibly due to binding ABT-737, would free proapoptotic proteins of the Bcl family such as Bax and Bak that are otherwise sequestered by Bcl-x_L. These would then be able to translocate to the cell mitochondria, inducing release of cytochrome *c* and triggering the apoptotic pathway. Details regarding the fit are presented in Supplementary Material, Section B2.

An age-structured model of carboplatin therapy

The cytotoxicity of carboplatin is primarily due to its interaction with nucleophilic N-7 sites of purine bases in DNA to form intrastrand adducts. This DNA damage is subsequently recognized by a number of candidate proteins such as the

Published OnlineFirst December 17, 2010; DOI: 10.1158/0008-5472.CAN-10-3174

Table 1. List of parameter values

Parameter	Value	Units	Source
λ_n	1.3713	Per day	11, 19[a]
β_0	1.4017	Per day	11[b]
b_0	0.22×10^{-3}	μM Bcl-x_L per cell	11, 19[b]
ν	1.7404	Dimensionless	11, 19[b]
α_0	1.9762	Per day	11[b]
C_0	60	μM carboplatin	11[b]
ρ_0	3.79×10^{-3}	Per day per μM carboplatin	11[b]
ρ_1	99	Per day per μM carboplatin	11[b]
b_l	0.1494×10^{-3}	μM Bcl-x_L per cell	11[b]
κ	1,700	Dimensionless	11[b]
$\in$	0.01	Days	11[b]
a_0	1.4	Days	11[b]
θ	3.4486	Dimensionless	11[b]
b_s	0.15×10^{-3}	μM Bcl-x_L per cell	27, 28, 29, 30[c]
λ_c	0.1676	Per day	31
λ_b	1.0397	Per day	32, 33[c]
γ_0	0.31×10^{-3}	μM Bcl-x_L per cell per day	[d]
k_1	86.4	Per μM protein per day	27[e]
k_{-1}	86.4	Per day	12, 34[f]
λ_x	0.4632	Per day	35[g]
a_r	2	Days	11

[a]In the absence of values in the literature, biologically realistic values for these parameters were chosen so that the solution profiles best fit experimental observation as described in refs. 11 and 19.

[b]In the absence of data, intracellular expression of Bcl-x_L was taken to be similar to that of Bcl-2 (IGROV-1 cells are known to express only Bcl-x_L and not Bcl-2; ref. 11). Typical expression of Bcl-2 in cells is ~75 nmol/L (28). However, much of this is sequestered by the proapoptotic members of the Bcl family such as Bax and Bid. Typical expression levels of these are in the range of 200 to 600 nmol/L Bax (29) and 25 nmol/L Bid (28), respectively. Furthermore, the dissociation constant for Bcl-2 binding with proapoptotic proteins in the Bcl family can be as low as 0.6 nmol/L (30). Using reaction rates for Bcl-2 binding to Bax taken from ref. 27, we get that free Bcl-2 concentrations can range from 0.008 to 0.3 nmol/L per cell. Therefore, a value of 0.15 nmol/L lying between these two limits was chosen to represent the free Bcl-x_L expression levels in IGROV-1 cells.

[c]The half-life of Bcl-x_L was assumed to be similar to that of Bcl-2. This has a reported value of between 12 and 20 hours; therefore, a mean value of 16 hours is chosen.

[d]The rate of Bcl-x_L production is chosen so that all cells constitutively express b_S amount of free Bcl-x_L. This gives $\gamma_0 = 2\lambda_b b_s$.

[e]It was assumed that the rate of forward reaction of ABT-737 with Bcl-x_L was similar to that of Bax binding to Bcl-2 because of their comparable binding affinities.

[f]The binding affinity of ABT-737 with Bcl-x_L is ~1 nmol/L.

[g]The half-life of ABT-737 in culture medium is taken to be the same as that of 072RB, another small molecule inhibitor of the Bcl-family. It should be noted that the range of half-lives of other small molecule inhibitors such as sHA-14-I and Su5416 also has similar reported values.

nonhistone chromosomal high-mobility groups 1 and 2. This results in the activation of a number of downstream pathways that could eventually lead to cell-cycle arrest, followed by a decision to survive or undergo apoptosis based on the extent and hence reparability of DNA damage. Many mechanisms related to these pathways remain to be elucidated (21).

To model these effects of application of carboplatin therapy on IGROV-1 cells, an additional compartment is added to the cell population, a schematic of which is presented in Fig. 1C. Upon drug application, the proliferating cells will undergo cell-cycle arrest at a certain rate dependent on the amount of therapy administered. A Hill-like functional form with Hill coefficient 1 is chosen to represent this rate (see Supplementary Material, Section B3), as it makes the biologically realistic assumption that when carboplatin concentration is zero, there will be no change in DNA integrity. As the amount of drug applied increases, the rate of cell-cycle arrest increases because of increasing levels of DNA damage, up to a maximum level. Furthermore, this profile also matches the cell proliferation assays as described in ref. 11, wherein carboplatin-induced cell growth inhibition was reported to follow a Hill function curve.

The arrested cells are removed to a separate compartment, where the cells will undergo apoptosis or will recover to the proliferating population. An age structure is imposed on the cells in this compartment to reflect the time taken from induction of DNA damage to eventual cell death or recovery.

Published OnlineFirst December 17, 2010; DOI: 10.1158/0008-5472.CAN-10-3174

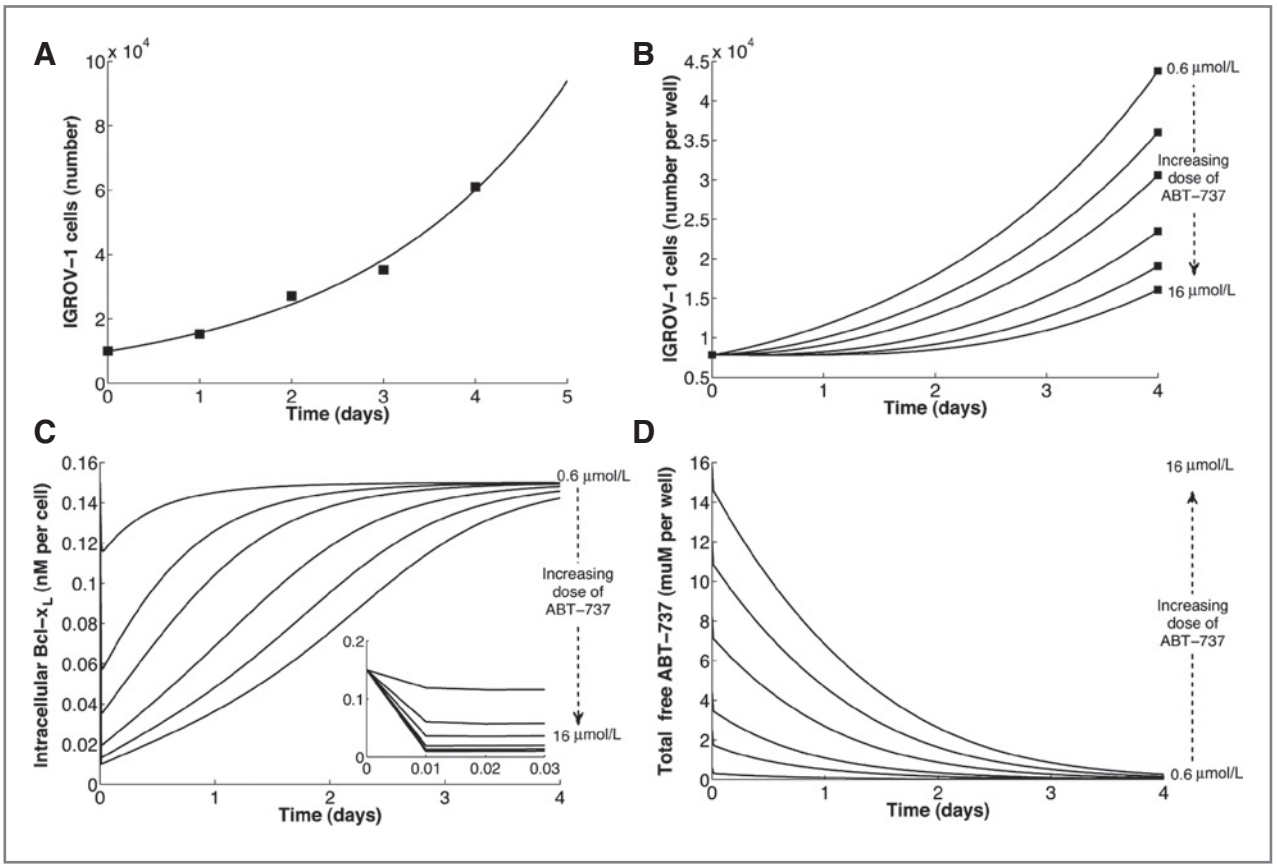

Figure 2. Fit to control and ABT-737-only therapy. A, IGROV-1 proliferation rate is estimated by fitting the model as described in Fig. 1A to daily counts of IGROV-1 cells cultured in the presence of growth medium alone (19). B, for the case when ABT-737 is administered to IGROV-1 cell cultures, the model is modified according to that described in Fig. 1B. This is subsequently fit to cell growth and survival assays, as that described in ref. 11, wherein cells are treated with varying amounts of ABT-737 and level of growth inhibition recorded 4 days hence. C and D, corresponding to various doses of ABT-737 in B, intracellular Bcl-x_L (in nanomoles per liter per cell, C) and total free ABT-737 (in micromoles per liter per well, D) are shown. Upon therapy, Bcl-x_L levels drop very rapidly (inset, C) and recover at a rate dependent on the quantity of ABT-737 delivered. Black squares, experimental data.

Models of chemotherapy have previously incorporated an age structure that is imparted to the equations governing cell growth, as it progresses through the cell cycle (22, 23). However, it is known that carboplatin is not cell-cycle specific and affects cells in all stages of the cell cycle (24). Thus, in our model, we do not distinguish between the various phases of cell growth. To the best of our knowledge, this is the first time that an age structure has been applied to a model of platinum-based chemotherapy wherein the age of arrested cells is tracked to mimic the experimentally observed delay in the onset of apoptosis from the time of cell arrest.

It has been experimentally determined that cell cytotoxicity is linearly correlated with the amount of platinum bound to the DNA and hence the extent of DNA damage (21). This is reflected in our choice of the rate of arrested cell death. This is taken to be function of age a of the arrested cell and the amount of carboplatin at the time of cell-cycle arrest, $C(t-a)$. These cells begin dying at some characteristic age a_{char}, determined experimentally to be 48 hours in ref. 11. Cells are also allowed to recover to the proliferating population, as explained in Equation (B) of the Quick Guide. Both the rate of arrest of proliferating cells and the rate of arrested cell death are fit to *in vitro* cell growth inhibition data taken from ref. 11, wherein carboplatin therapy is applied singly to IGROV-1 cell cultures (see Fig. 3). Further details regarding the fits are presented in Supplementary Material, Section B3.

Finally, to simulate combination therapy, the two single-therapy modules must be combined appropriately. We first note that it has been experimentally shown that Bcl-x_L does not protect cells from undergoing cell-cycle arrest as a result of chemotherapy-induced DNA damage (8). We therefore propose the following model schematic, as shown in Fig. 1D. Carboplatin induces DNA damage leading to cell-cycle arrest and subsequent cell death, which might be accentuated by anti-Bcl-x_L therapy. This, of course, also has an effect on proliferating IGROV-1 cells and has been quantified earlier. In this case, we have two unknown functions that need to be determined—the time of onset of arrested cell death, which is now a function of intracellular Bcl-x_L (as opposed to a constant in the carboplatin-only case), and arrested cell death rate, which must also depend on intracellular Bcl-x_L in addition to arrested cell age and the amount of carboplatin at the time of cell-cycle arrest. The full set of equations modeling combination therapy is given in Supplementary Material, Section A.

Published OnlineFirst December 17, 2010; DOI: 10.1158/0008-5472.CAN-10-3174

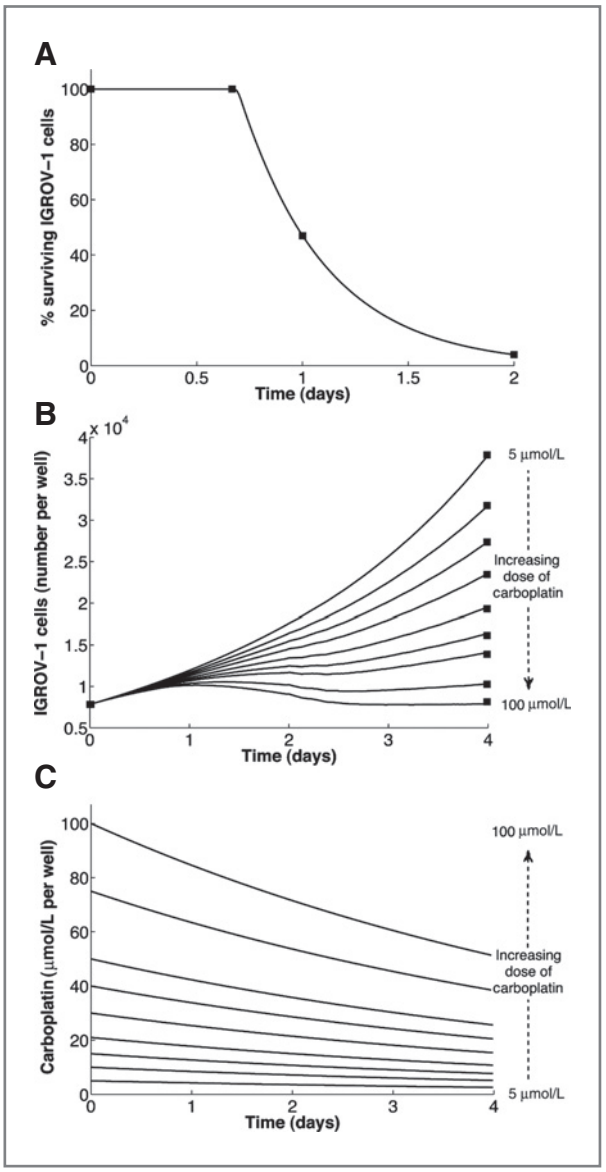

Figure 3. Fit to carboplatin-only therapy. A, upon carboplatin therapy, the percentage of IGROV-1 cells surviving was recorded over a period of 48 hours, as in experiments described in ref. 11. The death rate of arrested cells is estimated from these data as a function of carboplatin concentration and time from the application of therapy, and the resulting fit is shown. B, for the case when carboplatin is administered to IGROV-1 cell cultures, the model is modified according to that described in Fig. 1C. This is subsequently fit to cell growth and survival assays, as that described in ref. 11, wherein cells are treated with varying amounts of carboplatin and level of growth inhibition recorded 4 days hence. C, corresponding to various doses of carboplatin as described earlier, drug profiles (in micromoles per liter per well) as a function of time are shown. Black squares, experimental data.

Results

The two single-therapy modules as described in the preceding section are calibrated against *in vitro* cell proliferation assays as described in ref. 11, and the resulting fits shown in Figs. 2 and 3. Details regarding the fits and simulation methodology are available in the Supplementary Material. Figure 2 shows the simulations resulting from the application of ABT-737 alone. Figure 2B shows the best fit to the experimental data in terms of IGROV-1 cell number N at the end of 4 days of therapy. Figure 2C and D show the corresponding intracellular Bcl-x_L levels (b) and ABT-737 concentrations (X), respectively. It is observed that the application of therapy on day 0 causes a sharp decrease in the intracellular Bcl-x_L level. As the amount of drug delivered is increased, the cells take longer to recover their constitutive levels of Bcl-x_L expression, even though most of the free drug has degraded by this time.

Figure 3B shows the best fit to the experimental data in terms of total IGROV-1 cell number T at the end of 4 days of carboplatin therapy administered at day 0. Here, the death rate of arrested cells has already been estimated as described in Supplementary Materials and plotted in Fig. 3A. As can be seen, in agreement with experimental data, the arrested cells begin dying at around 16 hours posttherapy. Figure 3C shows the carboplatin concentration (C) for varying doses administered at day 0. Given the relatively low rate of carboplatin decay, even at the end of 4 days of therapy, the level of drug in cell culture assays remains high, indicating that the time period of action of a single dose of carboplatin is significantly longer than that of ABT-737.

Carboplatin treatment primes cells for anti-Bcl-x_L therapy

We begin our simulation of combination therapy by simulating a cell growth inhibition assay as described in ref. 11, wherein the amount of ABT-737 administered on day 0 was fixed at 0.6 μmol/L, which by itself would result only in a 6% to 7% growth inhibition after 4 days (Fig. 4C, solid circle and dashed line) as compared with the no-therapy control case (Fig. 4C, asterisk and dotted line). The amount of carboplatin coadministered was adjusted so that 50% growth inhibition was achieved by day 4. It was observed that 10 μmol/L carboplatin was required in addition to 0.6 μmol/L ABT-737 to achieve this. Administered without any ABT-737 cotreatment, 10 μmol/L carboplatin would induce only a 30% growth inhibition in the same period (Fig. 4C, solid triangle and dash-dotted line). Thus, the effect of combination therapy, assuming mutually independent action of the 2 drugs, is predicted to be only 37% growth inhibition. This implies that to simulate the observed synergism between the drugs, and given that anti-Bcl-x_L therapy does not affect the rate of carboplatin-induced cell-cycle arrest (8), the additional growth inhibition must be a result of enhanced arrested cell death rate because of ABT-737–induced lowering of intracellular Bcl-x_L b. This assumption is built into the model as depicted in Fig. 1D and quantified in our fits of arrested cell death rate (Fig. 4B) and time to onset of arrested cell apoptosis [$a_{char}(b)$; Fig. 4A]. Note that experimental data relating to relative timing of dosage of ABT-737 and carboplatin, as described in following sections, are also taken into account while conducting these fits. The resultant fit to cell growth inhibition data is shown in Fig. 4C. The model further predicts that in this scenario, most of the arrested cells undergo apoptosis and are extremely unlikely to recover to the proliferating population (data not shown).

Published OnlineFirst December 17, 2010; DOI: 10.1158/0008-5472.CAN-10-3174

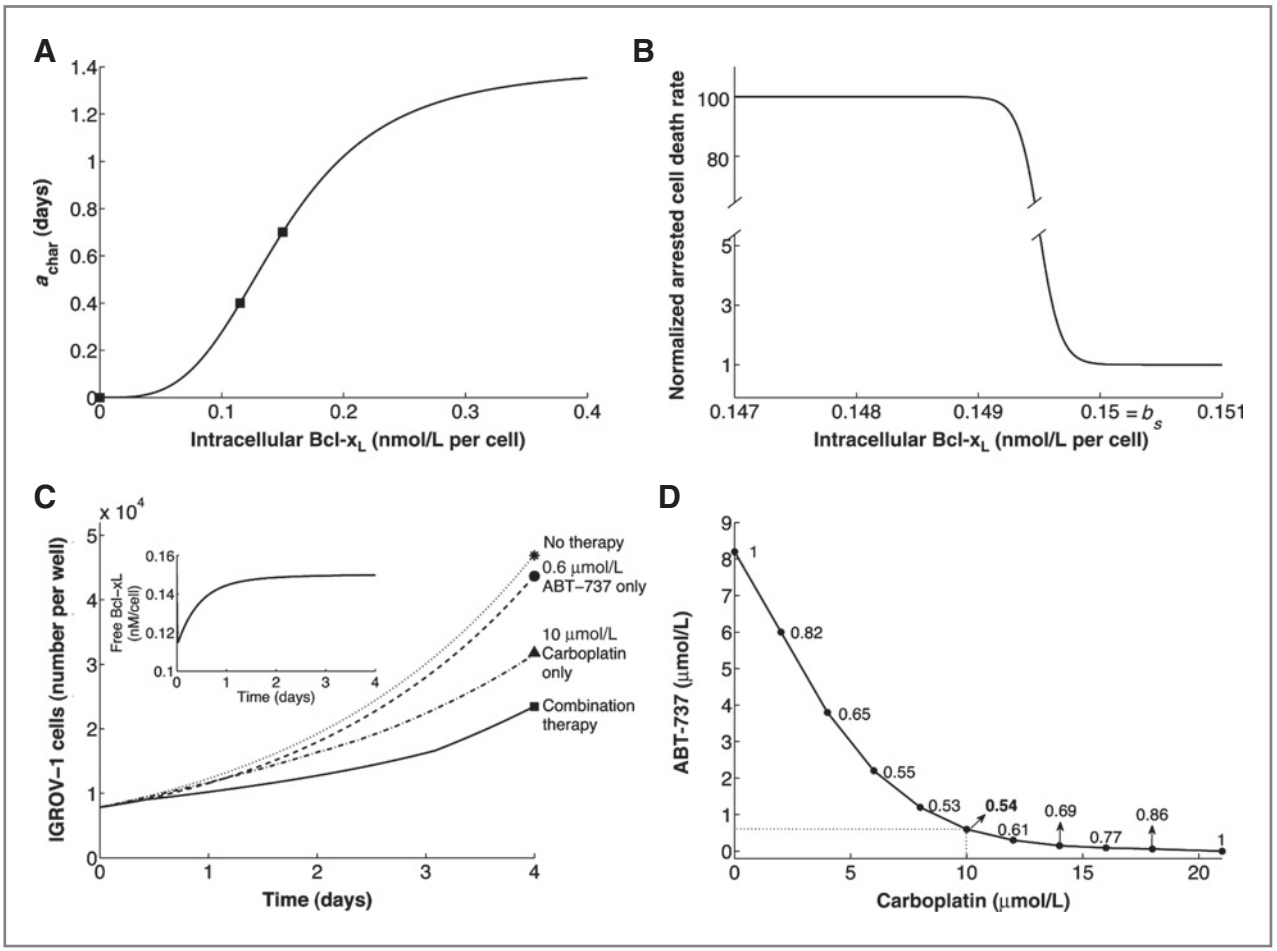

Figure 4. Combination therapy. A, in the case wherein IGROV-1 cells were cultured in the presence of both carboplatin and ABT-737, it was observed that the time of onset of arrested cell death was decreased (11). Hence, the dependence of this death rate on intracellular Bcl-x_L concentration is determined by fitting experimental data taken from ref. 11. Black squares, experimental data. B, in the case of combination therapy, the (normalized) maximum death rate of arrested cells is shown as a function of intracellular Bcl-x_L. The model is modified according to that described in Fig. 1D, and a fit is carried out to data shown in Figs. 4C and 5 in order to estimate the functional form of the Bcl-x_L–dependent death rate of arrested cells. The experimental data being fit is in the form of several combination indices based on scheduling of ABT-737 with respect to carboplatin therapy as reported in ref. 11. To match these data, it is necessary to assume that the arrested cells that have incurred DNA damage as a result of carboplatin therapy are extremely sensitive to changes in intracellular Bcl-x_L—if this level decreases by more than 1%, the cells will undergo apoptosis. C, an additional data point used to fit Bcl-x_L–dependent death rate of arrested cells is the 50% cell growth inhibition that results from coadministering 10 μmol/L carboplatin with 0.6 μmol/L ABT-737. Shown here is the resultant fit. Data point, black square; simulation, solid line. Inset, the effect of combination therapy on intracellular Bcl-x_L. Also plotted are the effects of giving these drug doses alone on IGROV-1 cell growth, with model simulations in dotted or dashed lines. D, simulations of the full model are carried out to obtain CI values (inscribed on the dosage curve) computed for a 50% desired cell kill for various combinations of carboplatin and ABT-737. Following the experimental protocol in ref. 11, it is assumed that both drugs are given simultaneously at day 0 and the level of growth inhibition of IGROV-1 cells recorded at day 4. The indicated value (dotted lines) is the experimental data point available from ref. 11. Simulations indicate that a combination of 1.2 μmol/L ABT-737 together with 8 μmol/L carboplatin maximizes the synergism between the 2 drugs.

ABT-737 impairs the ability of cells to recover from DNA damage

To fit experimental data relating to relative timing of ABT-737 and carboplatin application (shown in Fig. 5, last column, rows 1–5), a number of different functional forms were tried for arrested cell death rate (for details, see Supplementary Material, Section B4). In these experiments, carboplatin was administered to IGROV-1 cells in culture for 1 day, the cells were pre-, co-, or posttreated with 0.6 μmol/L ABT-737, and cell growth inhibition was recorded at day 4 (Fig. 5, as in ref. 11, solid boxes indicate all drug washed from cell culture). It was found that posttreatment with ABT-737 induced maximum level of synergism between the two drugs and was proposed as regimen of choice. The best fit to these data was obtained upon assuming that a greater than 1% fluctuation in the value of intracellular Bcl-x_L implies that the arrested cells will be unable to recover from DNA damage and consequently undergo apoptosis (Fig. 4B). Note that the experimental data point in the last column of row 5 (Fig. 5) does not match with our model simulations (penultimate column, row 5). This is discussed in further detail in the next section.

Published OnlineFirst December 17, 2010; DOI: 10.1158/0008-5472.CAN-10-3174

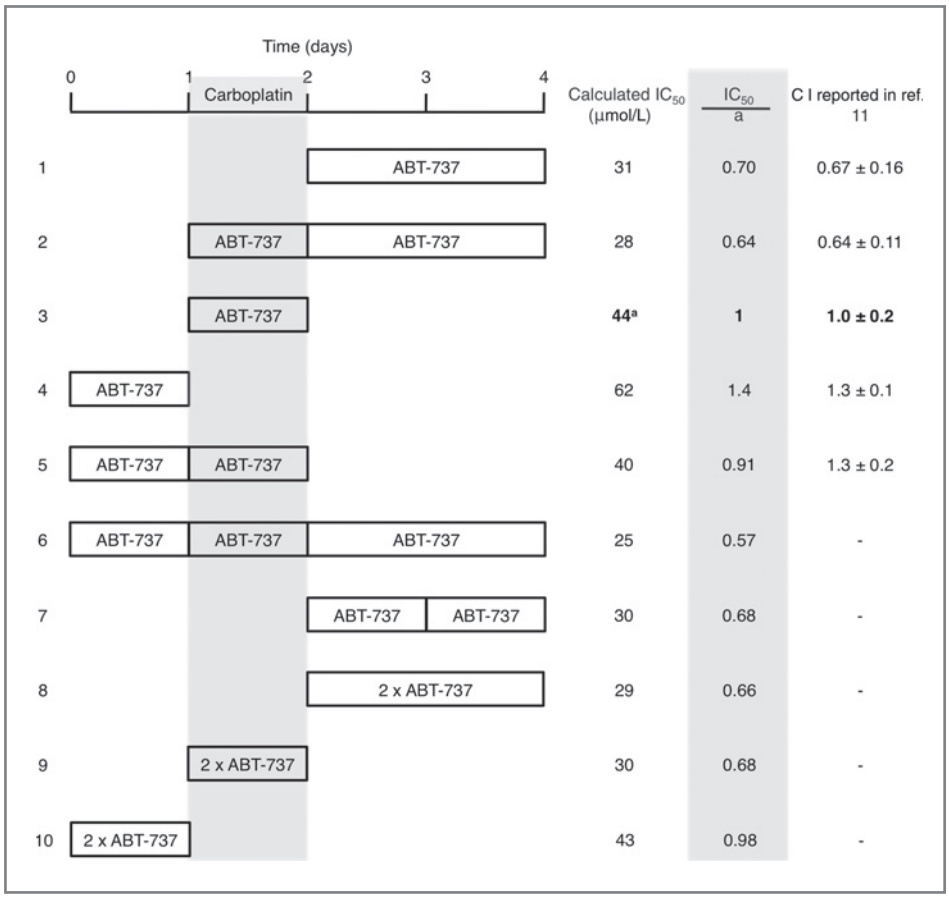

Figure 5. Scheduling of ABT-737. IGROV-1 cells are treated with a range of concentrations of carboplatin for a period of 24 hours and pretreated, cotreated, or posttreated with 0.6 or 1.2 μmol/L ABT-737. Following the convention in ref. 11, rectangular boxes indicate the addition of new drug and removal of any drug previously added. Carboplatin is administered on day 1 and removed 24 hours later. Combination indices (CI; last column) are computed for a 50% desired cell kill, as reported in ref. 11 and are used to fit the full model system as in Fig. 1D describing combination therapy. For the various dosing regimens, IC_{50} of carboplatin as estimated numerically is reported in micromoles per liter values. For comparison with experimental CI values, a ratio of the various IC_{50} values with that from schedule number 3 ($a = 44$ μmol/L) is used, as this has a reported CI of 1 and therefore regarded as the baseline. In general, there is a good agreement with the experimental data. Simultaneous treatment and posttreatment with ABT-737 are predicted as the best therapeutic strategy that fully exploits the basis of synergism between the 2 therapies in the case when the total dose of ABT-737 is fixed at 1.2 μmol/L.

Optimal dose scheduling regimens

Having extensively calibrated and fitted our model, we can now use it to investigate in detail the levels of synergism predicted for various dose-scheduling regimens. Following the experimental protocol laid down in ref. (11), we take as an indication of level of synergism a ratio of the predicted carboplatin concentration required to obtain 50% cell growth inhibition when combined with 1 to 3 doses of ABT-737 each of 0.6 μmol/L, with the control case, wherein the cells are cotreated with both drugs for 24 hours (row 3). A ratio of 1 or greater indicates suboptimal dosing, whereas a ratio of less than 1 indicates optimal dosing. (Combination indices calculated as described in ref. 25. See Supplementary Material, Section D for an explanation of these calculations.) Therefore, to find an optimal schedule, we need to minimize the amount of carboplatin required, for a given fixed amount of ABT-737 administered, to achieve a desired cell-kill fraction, by varying the timing of administering the two drugs with respect to each other. As can be seen from the first 5 rows of Fig. 5, the experimental data and model simulations both predict that pretreatment of IGROV-1 cells with ABT-737 is a suboptimal strategy. However, the true usefulness of the model lies in the ability to test dosing regimens suggested by but yet untested in experiments and which would take a very long time if carried out. Simulation indicates that cotreatment, followed by immediate posttreatment with ABT-737, indicates greater therapeutic benefit than purely posttreatment (row 2 vs. rows 7 and 8). This is also a better strategy than simply cotreatment but with double dose of ABT-737 (row 9). Finally, pretreatment in all but case 6 (rows 4, 5, and 10) seems to do worse as compared with any strategy that avoids pretreatment. Thus, in agreement with experimental results, the model predicts that if only a single dose of ABT-737 may be given in combination with carboplatin therapy, posttreatment is the best option (row 1). However, if 2 doses of ABT-737 are allowed, the best strategy is predicted to be cotreatment, immediately followed by posttreatment (row 2). Note that in row 6, as 3 doses of ABT-737 are being delivered, best results are predicted. In fact,

Published OnlineFirst December 17, 2010; DOI: 10.1158/0008-5472.CAN-10-3174

if 3 doses of ABT-737 are allowed, the model predicts that 1 to 2 doses must be given post–carboplatin treatment; the timing of the third dose is relatively flexible (not shown). Therefore, in all cases, posttreatment with ABT-737 is indicated.

Prediction of optimal relative dosages

Finally, we turn our attention to a key question that arises in the chemotherapeutic treatment of cancers—"What should the relative dose sizes of two (or more) drugs be, in order to maximize tumor cell exposure, while minimizing the amount of drugs administered?" Figure 4D is a phase diagram showing the amounts of carboplatin and ABT-737 required to achieving a desired cell growth inhibition of 50% when these two drugs are administered simultaneously. Here, minimizing patient drug load is equivalent to minimizing their CI. (Note: We are attempting to minimize the following function, subject to the condition that after 4 days, cell numbers in culture should be half the value in the case when no therapy is given. $\mathrm{CI} = \frac{\mathrm{C}(0)}{\mathrm{C}_{50}} + \frac{\mathrm{X}(0)}{\mathrm{X}_{50}}$. Here, $C(0)$ and $X(0)$ are the doses of carboplatin and ABT-737 administered at time $t = 0$; C_{50} and X_{50} are the amounts of the two drugs required to achieve 50% growth inhibition when administered singly; $C(0)$ is allowed to vary between 0 and C_{50} and the constraint used to generate values of $X(0)$. This may be regarded as an optimization problem in a single variable $C(0)$ that takes values on a closed interval and therefore attains its minimum therein.) A computation of the CI for each pair of doses is enumerated along the dose curve. A combination of 8 μmol/L carboplatin together with 1.2 μmol/L ABT-737 is predicted to optimize the synergism between the 2 drugs. Such phase diagrams can similarly be computed for any desired cell kill.

Discussion

In this article, we presented a model of combination chemotherapy comprising the platinum-based drug carboplatin, together with a novel small molecule inhibitor ABT-737, in the case of ovarian carcinomas. To elucidate the mechanism of interaction between the 2 drugs, details of the apoptotic pathway were incorporated at a molecular level and a cell age structure was applied to simulate the effect of DNA damage on cell fate. The model was extensively calibrated against experimental data and subsequently used to make key predictions regarding dose and schedule optimization that arise in the field of cancer chemotherapeutics.

The model could verify the experimentally proposed hypothesis that carboplatin sensitizes cancer cells for treatment with ABT-737. In fact, it explicitly emerged from our simulations that the principal reason for this is the reduced ability of DNA-damaged cells to withstand changes in intracellular Bcl-x_L concentration. In addition, a hypothesized reduction in the time of onset of arrested cell death as a result of coadministration of ABT-737 with carboplatin was predicted to have limited impact on cell growth inhibition and therefore on synergism between the 2 drugs. The model further predicted the existence of a threshold for intracellular Bcl-x_L concentration below which carboplatin-treated cells are unable to survive.

It has been proposed that insufficient exposure of tumor cells to drugs could contribute to chemoresistance development, calling for a need to conduct studies aimed at optimizing chemotherapeutic schedules (26). However, such studies have typically high financial as well as human costs. Using modeling such as that presented here to arrive at principles of optimal dose scheduling can lead to significant cost savings and faster clinically applicable results. For instance, for a maximum of 2 fixed doses of ABT-737 and a single dose of carboplatin, we predicted that cotreatment immediately, followed by posttreatment of ABT-737 with carboplatin, was the best strategy. In fact, such regimens can easily be computed for any given number of doses of the 2 drugs to be administered over a given length of time. Likewise, fixing the target cell kill at 50%, we were able to predict dose sizes of these 2 drugs to be coadministered in order to optimize their synergism and hence minimize patient drug load. Such phase diagrams can also be computed for any desired cell kill to minimize drug dose or under a constraint on the maximum tolerated amount of each drug to maximize cell kill. Although this is, of course, not intended to replace clinical testing, it can minimize the various choices that need to be examined experimentally, in addition to being a quantitative tool useful for interpreting experimental results.

Relative dose scheduling experiments reported in ref. 11 suggest that pretreatment of IGROV-1 cells with ABT-737, followed by cotreatment with carboplatin and ABT-737, is suboptimal (Fig. 5, row 5, last column). However, this is in contradiction to the additive effect predicted when cells are simply cotreated with the 2 drugs (Fig. 5, row 3, last column), as in the previous case, one is starting with fewer cells at the time of cotreatment. Our model predicted a near-additive effect in both cases, and an experiment such as that suggested in row 6 of the same figure, where pre-, co-, and posttreatment is carried out, would help to understand this apparent discrepancy.

The model presented here was conscientiously fit to relevant experimental data and a balance between incorporating the maximum possible biological details and keeping unknowns to a minimum was striven for. The simplicity of the model, combined with good agreement between numerical simulations and experimental data, suggests that it may be a valuable tool for hypothesis generation. However, the quality of the model predictions will have to be verified in further experiments. For instance, instead of recording cell growth inhibition in response to the various therapies at the end of 4 days, it would be extremely useful to maintain a daily cell count record. This could then be used to fine-tune the proliferating cell death rate, rate of cell arrest, and most important, a rate for cell recovery from DNA damage (which is taken in to occur spontaneously after a certain length of time in our model due to a lack of such data). A measure of the constitutive levels of expression of some of the key players in the Bcl family, especially Bcl-x_L, would help to precisely quantify the effect of ABT-737 on DNA-damaged cells. Then, simulations of the predicted effect of the therapies could be carried out with confidence on any given cell line. The input data required would only be a comparison of the level of

Published OnlineFirst December 17, 2010; DOI: 10.1158/0008-5472.CAN-10-3174

expression of such proteins, which could be obtained by methods such as Western blotting. The model described in this article has the potential of developing into a valuable quantitative tool to aid in the translation of drugs such as ABT-737 from the experimental to clinical settings and underscores the need for close collaboration between modeling and simulation efforts and experimentalists. Given the high costs of drug development, such collaborations can have a far-reaching impact on the field of cancer therapeutics.

Disclosure of Potential Conflicts of Interest

No potential conflicts of interest were disclosed.

Acknowledgments

The authors gratefully acknowledge the feedback and comments of Prof. Helen Byrne.

Grant Support

H.V. Jain was supported by the National Science Foundation Award (0635561). M. Meyer-Hermann was supported by the EU-NEST project MAMOCELL in FP6 and by the BMBF GerontoMitoSys project. FIAS was supported by the ALTANA AG.

The costs of publication of this article were defrayed in part by the payment of page charges. This article must therefore be hereby marked *advertisement* in accordance with 18 U.S.C. Section 1734 solely to indicate this fact.

Received August 26, 2010; revised November 11, 2010; accepted December 6, 2010; published OnlineFirst December 17, 2010.

References

1. Roett MA, Evans P. Ovarian cancer: an overview. Am Fam Physician 2009;80:609–16.
2. Despierre E, Lambrechts D, Neven P, Amant F, Lambrechts S, Vergote I. The molecular genetic basis of ovarian cancer and its roadmap towards a better treatment. Gynecol Oncol 2010;117:358–65.
3. Vasey PA. Resistance to chemotherapy in advanced ovarian cancer: mechanisms and current strategies. Br J Cancer 2003;89 Suppl 3: S23–8.
4. Stewart DJ. Mechanisms of resistance to cisplatin and carboplatin. Crit Rev Oncol Hematol 2007;63:12–31.
5. Adams JM. Ways of dying: multiple pathways to apoptosis. Genes Dev 2003;17:2481–95.
6. Williams J, Lucas PC, Griffith KA, Choi M, Fogoros S, Hu YY, et al. Expression of Bcl-xL in ovarian carcinoma is associated with chemoresistance and recurrent disease. Gynecol Oncol 2005;96:287–95.
7. Liu JR, Fletcher B, Page C, Hu C, Nunez G, Baker V. Bcl-xL is expressed in ovarian carcinoma and modulates chemotherapy-induced apoptosis. Gynecol Oncol 1998;70:398–403.
8. Minn AJ, Rudin CM, Boise LH, Thompson CB. Expression of Bcl-xL can confer a multidrug resistance phenotype. Blood 1995;86:1903–10.
9. Villedieu M, Louis MH, Dutoit S. Absence of Bcl-xL down-regulation in response to cisplatin is associated with chemoresistance in ovarian carcinoma cells. Gynecol Oncol 2007;105:31–44.
10. Brotin E, Meryet-Figuière M, Simonin K, Duval RE, Villedieu M, Leroy-Dudal J, et al. Bcl-xL and MCL-1 constitute pertinent targets in ovarian carcinoma and their concomitant inhibition is sufficient to induce apoptosis. Int J Cancer 2010;126:885–95.
11. Witham J, Valenti MR, De-Haven-Brandon AK, Vidot S, Eccles SA, Kaye SB, et al. The Bcl-2/Bcl-xL family inhibitor ABT-737 sensitizes ovarian cancer cells to carboplatin. Clin Cancer Res 2007;13:7191–8.
12. Oltersdorf T, Elmore SW, Shoemaker AR, Armstrong RC, Augeri DJ, Belli BA, et al. An inhibitor of Bcl-2 family proteins induces regression of solid tumours. Nature 2005;435:677–81.
13. Stauffer SR. Small molecule inhibition of the Bcl-X(L)-BH3 protein-protein interaction: proof-of-concept of an *in vivo* chemopotentiator ABT-737. Curr Top Med Chem 2007;7:961–5.
14. Kempf H, Bleicher M, Meyer-Hermann M. Spatio-temporal cell dynamics in tumour spheroid irradiation. Eur Phys J D 2010;60:177–93.
15. Schaller G, Meyer-Hermann M. Continuum versus discrete model: a comparison for multicellular tumour spheroids. Philos Trans A Math Phys Eng Sci 2006;364:1443–64.
16. Schaller G, Meyer-Hermann M. Multicellular tumor spheroid in an off-lattice Voronoi-Delaunay cell model. Phys Rev E Stat Nonlin Soft Matter Phys 2005;71:051910.
17. Jain HV, Nör JE, Jackson TL. Quantification of endothelial cell-targeted anti-Bcl-2 therapy and its suppression of tumor growth and vascularization. Mol Cancer Ther 2009;8:2926–36.
18. Jain HV, Nör JE, Jackson TL. Modeling the VEGF-Bcl-2-CXCL8 pathway in intratumoral angiogenesis. Bull Math Biol 2008;70:89–117.
19. Bottero F, Tomassetti A, Canevari S, Miotti S, Ménard S, Colnaghi MI. Gene transfection and expression of the ovarian carcinoma marker folate binding protein on NIH/3T3 cells increases cell growth *in vitro* and *in vivo*. Cancer Res 1993;53:5791–6.
20. Levine HA, Sleeman BD, Nilsen-Hamilton M. A mathematical model for the roles of pericytes and macrophages in the initiation of angiogenesis. I. The role of protease inhibitors in preventing angiogenesis. Math Biosci 2000;168:77–115.
21. Siddik ZH. Cisplatin: mode of cytotoxic action and molecular basis of resistance. Oncogene 2003;22:7265–79.
22. Basse B, Ubezio P. A generalised age- and phase-structured model of human tumour cell populations both unperturbed and exposed to a range of cancer therapies. Bull Math Biol 2007;69:1673–90.
23. Spinelli L, Torricelli A, Ubezio P, Basse B. Modelling the balance between quiescence and cell death in normal and tumour cell populations. Math Biosci 2006;202:349–70.
24. Nguyen HN, Sevin BU, Averette HE, Perras J, Ramos R, Donato D, et al. Cell cycle perturbations of platinum derivatives on two ovarian cancer cell lines. Cancer Invest 1993;11:264–75.
25. Chou TC, Talalay P. Quantitative analysis of dose-effect relationships: the combined effects of multiple drugs or enzyme inhibitors. Adv Enzyme Regul 1984;22:27–55.
26. Tan DS, Ang JE, Kaye SB. Ovarian cancer: can we reverse drug resistance? Adv Exp Med Biol 2008;622:153–67.
27. Chen C, Cui J, Zhang W, Shen P. Robustness analysis identifies the plausible model of the Bcl-2 apoptotic switch. FEBS Lett 2007;581:5143–50.
28. Hua F, Cornejo MG, Cardone MH, Stokes CL, Lauffenburger DA. Effects of Bcl-2 levels on Fas signaling-induced caspase-3 activation: molecular genetic tests of computational model predictions. J Immunol 2005;175:985–95.
29. Kuwana T, Mackey MR, Perkins G, Ellisman MH, Latterich M, Schneiter R, et al. Bid, Bax, and lipids cooperate to form supramolecular openings in the outer mitochondrial membrane. Cell 2002;111:331–42.
30. Wang S, Yang D, Lippman ME. Targeting Bcl-2 and Bcl-xL with non-peptidic small-molecule antagonists. Semin Oncol 2003;30:133–42.
31. Di Pasqua AJ, Goodisman J, Kerwood DJ, Toms BB, Dabrowiak JC. Modification of carboplatin by Jurkat cells. J Inorg Biochem 2007;101:1438–41.
32. Blagosklonny MV, Alvarez M, Fojo A, Neckers LM. bcl-2 protein downregulation is not required for differentiation of multidrug resistant HL60 leukemia cells. Leukoc Res 1996;20:101–7.
33. Eischen CM, Packham G, Nip J, Fee BE, Hiebert SW, Zambetti GP, et al. Bcl-2 is an apoptotic target suppressed by both c-Myc and E2F-1. Oncogene 2001;20:6983–93.
34. Mohammad RM, Goustin AS, Aboukameel A, Chen B, Banerjee S, Wang G, et al. Preclinical studies of TW-37, a new nonpeptidic small-molecule inhibitor of Bcl-2, in diffuse large cell lymphoma xenograft model reveal drug action on both Bcl-2 and Mcl-1. Clin Cancer Res 2007;13:2226–35.
35. Ponassi R, Biasotti B, Tomati V, Bruno S, Poggi A, Malacarne D, et al. A novel Bim-BH3-derived Bcl-xL inhibitor: biochemical characterization, *in vitro*, *in vivo* and *ex-vivo* anti-leukemic activity. Cell Cycle 2008;7:3211–24.

AACR American Association for Cancer Research

Cancer Research

The Journal of Cancer Research (1916–1930) | The American Journal of Cancer (1931–1940)

The Molecular Basis of Synergism between Carboplatin and ABT-737 Therapy Targeting Ovarian Carcinomas

Harsh Vardhan Jain and Michael Meyer-Hermann

Cancer Res 2011;71:705-715. Published OnlineFirst December 17, 2010.